

AUTOMATIC EXTRACTION OF SHADOW AND NON-SHADOW LANDSLIDE AREA FROM ADS-40 IMAGE BY STRATIFIED CLASSIFICATION

Yi-Ta Hsieh¹, Shou-Tsung Wu², Chen-Sung Liao³, Yau-Guang Yui^{#4}, Jan-Chang Chen⁵, Yuh-Lurng Chung^{#6}

¹ Department of Graduate Institute of Bioresources, National Pingtung University of Science and Technology
No.1, Shuehfu Rd., Neipu, Pingtung, 91201 Taiwan.

blue@gisfore.edu.tw

² Department of Tourism Management, Shih Chien University
No.200 University Rd., Neimen, Kaohsiung 84550, Taiwan

st.wu@msa.hinet.net

³ Department of Tropical Agriculture and International Cooperation, National Pingtung University of Science and Technology
No.1, Shuehfu Rd., Neipu, Pingtung, 91201 Taiwan

egg19870702@hotmail.com

[#] Department of Forestry, National Pingtung University of Science and Technology
No.1, Shuehfu Rd., Neipu, Pingtung, 91201 Taiwan

y10324@hotmail.com

cyl@gisfore.npust.edu.tw

⁵ Department of Recreation Management, Shih Chien University
No.200 University Rd., Neimen, Kaohsiung 84550, Taiwan

5zzz.john@msa.hinet.net

Abstract—The objective of this study is fast and accurate to detect the landslides automatically from shadow areas and non-shadow areas that use ADS-40 airborne multispectral image by stratified classification method. First, the shadow area was detected by the brightness method. The shadow and non shadow images were calculated Normalized Difference Vegetation Index (NDVI), and we used iterative self-organizing data analysis technique (ISODATA) unsupervised classification to classify the area of vegetation and non-vegetation. The highest overall classification accuracy of shaded and non-shaded Landslides was 85.75% and 92.75%, respectively. The classification of shaded area by 12-bit image radiation information has a certain capacity. This automated process can be effectively and quickly obtain information of Landslide.

Keywords—ADS-40, landslide, shadow, stratified classification

I. INTRODUCTION

Sediment disasters happened very frequently in Taiwan. Landslides and debris flows often seriously endanger the lives of people and the enormous property damage in mountainous regions. Therefore, it is important to monitoring landslide. Previous landslide mapping carried out by interpretation of stereoscopic aerial photographs ^{[5], [8]}, it can get accurately mapping results, but it takes a lot of manpower and time.

Remote sensing techniques have been successfully applied to landslide investigations, and investigators have attempted to use satellite images to identify and map landslides using digital image analysis ^{[6], [7]}.

For optical remote sensing is affected by shadows, it is difficult to extract the information of shadow region. In most of the cases, the shadows are considered as a nuisance ^[11]. And due to the interpretation of the shadow areas is difficult, the shaded area of the landslide is often ignored in the landslide interpretation procedures. Thus many landslides area were underestimated in the process of mapping. In few studies, how to detent landslides area of shadow area for optical remote sensing data have been evaluated. Recently, digital photogrammetric technology can achieve high spatial resolution, multi-spectral, 12-bit high radiometric resolution aerial image, like ADS-40, Z/I DMC, and those airborne sensors offer some potential for the landslide interpretation of shaded area.

The study aims to detect the landslides quickly and accurately from shadow areas and non-shadow areas by stratified classification method and via ADS-40 airborne multispectral images.

II. STUDY SITE AND MATERIALS

The study area is located in the Nantou county, central Taiwan, between 23°54' and 24°15' N, and between 121°13' and 121°15' E (Fig. 1).

Airborne multispectral image sets were acquired with the Leica ADS-40 system, which is production of LEICA Geosystems (www.gis.leica-geosystems.com). The ground resolution element of the ADS-40 multispectral imagery is 0.25 m, with 12-bit radiometric depth, and the DN value is a range from 0-4095. The ADS-40 used in this study comprised four spectral bands; visible red 610-660 nm, visible green 535-585 nm, visible blue 430-490 nm, and near infrared 835-885 nm. For the study area, with shadow and shadow-free aerial images were available. The two dates of ADS-40 image sets for shadow-free image and shadow image were collected by Aerial Survey Office of Taiwan on 21 September 2008 and on 27 December 2008, respectively. With shadow image (2008/12/27) was used for image digital analysis, and shadow-free image (2008/9/21) was used for validation of the shadow area landslide.

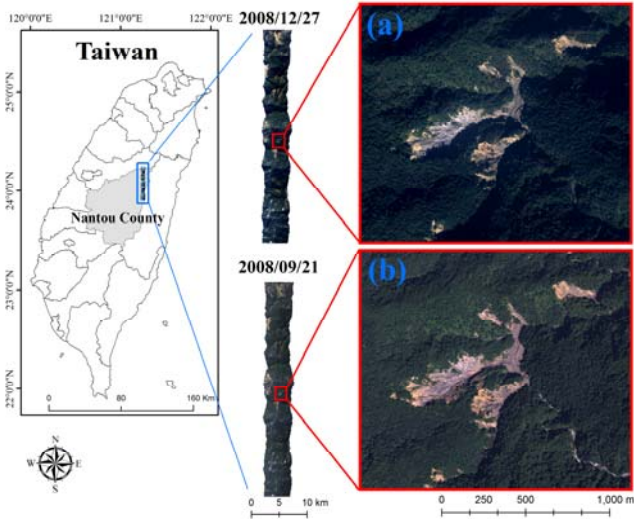


Fig.1. Study site and two date of images. (a), was with shadow image, which was collected on 27 December 2008, it was used for image digital analysis; (b), was shadow-free image, which was collected on 21 September 2008, it was used for validation of the shadow area landslide.

III. METHODS

In this study, stratified classification was applied to perform the detection of shadow and non-shadow landslide. The classification process is as follows.

A. Shadow detection

We applied a histogram thresholding method for shadow detection. The principle of a histogram thresholding method is based on the intensity difference of shaded and non-shaded areas [11]. In this study, we used the brightness method, which was defined as the mean of the four multispectral bands -red, green, blue, and near infrared to determine the threshold value. The brightness is calculated using the following equation:

$$\text{Brightness} = \frac{R + G + B + NIR}{4} \quad (1)$$

where R is visible red band; G is visible green band; B is visible blue band; NIR is near-infrared band.

We separated shaded area from non-shaded area using brightness method, and the brightness threshold value was determined by bimodal histogram splitting method, which selects the threshold by identifying the value at the valley between the two peaks in the histogram as the threshold for shadows and non-shadows [2], [10]. After determining threshold value, the shaded image was separated from non-shaded image.

An accuracy assessment was performed for the shadow detection results. A stratified random sampling was performed to generate the random points for the shadow detection results. A total number of 300 random points were sampled. The user's accuracy, producer's accuracy, overall accuracy, and Kappa statistic were also calculated.

B. Landslide detection: Non-shaded area landslide

1) *Vegetation index enhancement*: In order to enhance the spectral characteristics differences between vegetation and non-vegetation, vegetation index enhancement technique was selected to help identify. Vegetation index enhancement technique was selected to help identify landslide area in non-shadow image. Normalized Difference Vegetation Index (NDVI) can be assessed whether the target being observed contains live green vegetation or not. It was the near-infrared and visible red light combination formula [10]. NDVI can enhance the spectral characteristics differences between vegetation and non-vegetation for analysis images. The non-shaded images were calculated by NDVI. And the NDVI is calculated using the following equation:

$$NDVI = \frac{NIR - R}{NIR + R} \quad (2)$$

where R and NIR stand for the spectral reflectance measurements acquired in the visible red and near-infrared regions, respectively. The NDVI itself thus varies between -1.0 and +1.0.

2) *ISODATA unsupervised classification*: To enhance the difference between vegetation and non-vegetation, using the NDVI is a feasible approach. However, in order to classify vegetation and non-vegetation, the threshold of NDVI needs to be chosen manually for various scenes. Avert this drawback, using unsupervised classification technique to classify the non-vegetation threshold of NDVI automatic. In this study, we used iterative self-organizing data analysis technique (ISODATA) unsupervised classification to classify the area of vegetation and non-vegetation. Using ISODATA to classify NDVI image into the 2, 3, 4 classes in the final output, respectively. The 3, 4 classes were derived to grouped non-vegetation class. The classification with maximum number of iterations set to 6, and the convergence threshold set to 0.95. The pixels were identified for each of the classes. Then, we

get the distribution of non-vegetation area as the preliminary non-shaded landslide map.

3) *Data filter*: After we got the preliminary non-shaded landslide map, the data filters were used to reduce the classification noise (like salt and pepper effects). This step is for eliminating commissions of the preliminary landslide detection. First, use of existing land use layers *to filter* out artificial building area, and to reduce the classification error. Differences in scale of remote sensing image affect the minimum size of visible landslides. In [4] study showed that the inventory's smallest landslide area is 39 -49 m²; and in [3] study showed that the inventory's smallest landslide area is 50 m². Therefore, the preliminary landslide can filter out smaller area. We also applied a minimum size of area filter. The minimum size of detected area was filtered out, and it was lower than 30m².

C. Landslide detection: shaded area

The shaded area landslide detection processes is the same as non-shaded area landslide detection processes. It was also using vegetation index enhancement (NDVI), and then using ISODATA unsupervised classification to classify the area of vegetation and non-vegetation. Finally, it was also applied data filters to eliminate commissions.

D. Accuracy assessment

An accuracy assessment was performed for the non-shaded and shaded area landslide results, respectively. A random sampling was performed to generate the random points for the detection results. The non-shaded area landslide results were validated by interpretation of analysis image (2008/12/27). The shadow-free image (2008/9/21) was used for validation of the shadow area landslide. An 800 random points were sampled for non-shaded (400 points) and shaded area landslide (400 points) results. The user's accuracy, producer's accuracy, overall accuracy, and Kappa statistic were also calculated.

IV. RESULTS AND DISCUSSIONS

A. Shadow detection

Figure 2.e shows the histogram of brightness (i.e., the mean of the four bands, red, green, blue and NIR) for the study site, we can see the distribution of histogram. There are two peaks in the histogram, and the valley between the two peaks in the histogram is the threshold for shadow and non-shadow areas. To distinguish the shadow and non-shadow areas, we set a threshold of brightness value. The threshold value of 1000 was determined by a bimodal histogram splitting method (Figure 2e). After the threshold value determined was set, and the shadow detection result was created (Figure 2b,d).

Table I shows an error matrix that was derived from the shadow detection results obtained from the brightness method. The overall accuracy is reached to 98.75%, and the Kappa statistic is 0.98. The result shows high accurate shadow detection. The bimodal histogram splitting method has been successfully applied to threshold for shadows and non-

shadows in many studies, and it provides a simple, robust way for threshold of shadow [9], [2], [1], [11]. We used the shadow and non-shadow images to detect landslide area at next step.

TABLE I
ERROR MATRIX FOR SHADOW DETECTION

Classified Data	Reference Data		User accuracy (%)
	Shadow	Non-shadow	
Shadow	197	3	98.50
Non-shadow	2	198	99.00
Producers accuracy (%)	98.99	98.51	
Overall accuracy: 98.75%; Kappa statistic: 0.98			

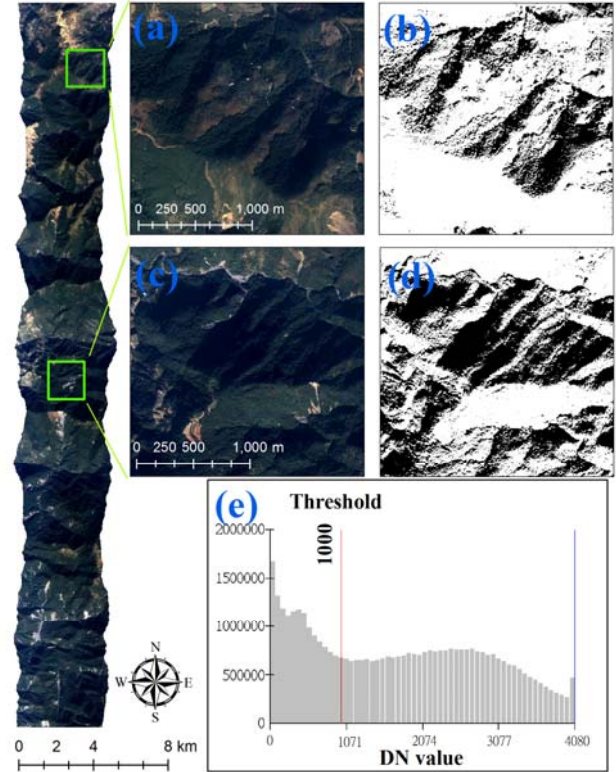


Fig.2. Shadow detection results. (a) and (c) represent shaded image; (b) and (d) represent shadow detection area with black color; (e), the histogram of brightness with 1000 threshold

B. Landslide detection

In this study, the goal is to achieve automatic classification for shadow and non-shadow images. The shadow and non shadow images were calculated by NDVI, and used ISODATA unsupervised classification to classify the area of vegetation and non-vegetation classes. We also tested effectiveness of different class number, in order to get the best classification result.

The non-shadow area landslide detection results indicate four classes ISODATA cluster (NSA-4) which is reached the highest accuracy. The accuracy overall of NSA-4 is 92.75%, and the Kappa statistic is 0.98. ISODATA threshold of NSA-4 is 0.33 (Table II). The result shows high accurate in non-shadow area landslide detection.

The shadow area landslide detection results also indicate four classes ISODATA cluster (SA-4) which is reached the

highest accuracy. The accuracy overall of SA-4 is 85.75%, and the Kappa statistic is 0.72. ISODATA threshold of NSA-4 is 0.56 (Table II). The non-shadow area landslide detection shows acceptable result. The classification of shaded area by 12-bit image radiation information has a certain capacity.

TABLE II
ACCURACY ASSESSMENT RESULTS

Methods	ISODATA threshold (NDVI)	Overall Accuracy (%)	Kappa	Producer's Accuracy (PA, %) and User's Accuracy (UA, %)			
				Non-landslide		Landslide	
				PA	UA	PA	UA
SA-2	0.84	84.71	0.70	97.35	72.06	77.02	97.95
NSA-2	0.59	90.25	0.81	99.42	81.90	83.26	99.47
SA-3	0.71	85.71	0.71	97.35	73.50	78.63	97.99
NSA-3	0.41	92.25	0.85	98.84	85.50	87.22	99.00
SA-4	0.56	85.75	0.72	97.35	73.50	78.71	98.00
NSA-4	0.33	92.75	0.86	99.42	86.00	87.67	99.50

SA=shadow area; NSA=non-shadow area; -2,-3,-4= class number of ISODATA classify

In Figure 3, the landslide detection maps of shaded and non-shadow that were overlay with shadow and shadow-free images. We can see that the landslide of the shaded region detection results is very reasonably (green cycle).

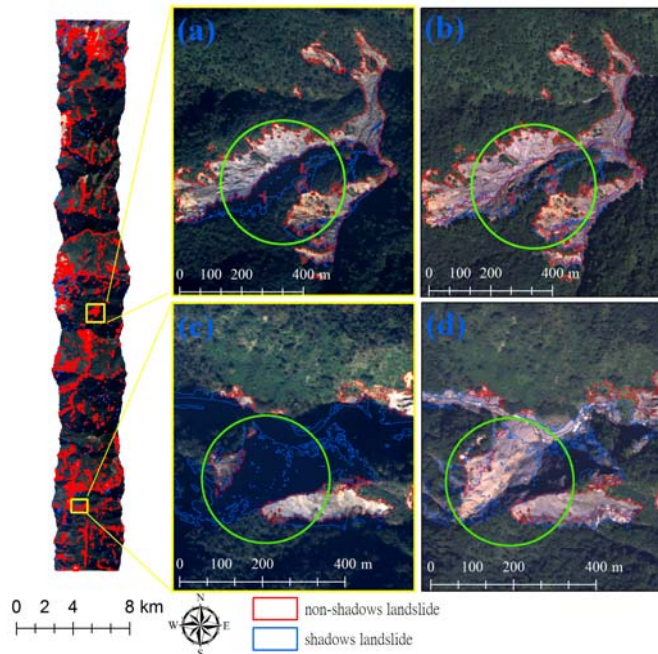


Fig.3 Landslide detection results. (a) and (c) are landslide detection results overlap the shaded image; (c) and (d) are landslide detection results overlap the shadow-free image.

This study showed that 12-bit image for the classification of the shaded area has potential, because of higher radiometric resolution. But we can note the shadow area of ISODATA threshold that seems show higher threshold than non-shadow area (Table II). In [11] study, they trying to classify between vegetation and artificial building in the shadow areas, where the shaded area using NDVI = 0.1 as the classification threshold, while in the non-shaded areas distinguish between vegetation and artificial building is used NDVI = 0.05 as the classification threshold, and results showed shaded area of vegetation classification threshold is higher than non-shaded situation. This study also obtained the same result. This means

the spectral of shadow and non-shaded areas with differences. The reasons need for further study.

V. CONCLUSION

The result shows high accurate shadow and non-shadow area landslide detection. The classification of shaded area by 12-bit image radiation information has a certain capacity. This automated process can effectively and quickly obtain information of shadow and non-shadow landslide.

ACKNOWLEDGEMENTS

The author would like to thank for Aerial Survey Office, Forestry Bureau providing ADS-40 multispectral image for this study.

REFERENCES

- [1] Y. Chen, D. Wen, L. Jing, and P. Shi, "Shadow information recovery in urban areas from very high resolution satellite imagery", *International Journal of Remote Sensing*, vol. 28 (15), pp. 3249-3254. 2007.
- [2] P. M. Dare, "Shadow analysis in high-resolution satellite imagery of urban areas", *Photogrammetric Engineering & Remote Sensing*, vol. 71(2), 169-177. 2005.
- [3] F. Imaizumi, R.C. Sidle, and R. Kamei, "Effects of forest harvesting on the occurrence of landslides and debris flows in steep terrain of central Japan", *Earth Surface Processes and Landforms* 33, 827-840. 2008.
- [4] F. Guzzetti, P. Aleotti, B. D. Malamud, and D. L. Turcotte, "Comparison of three landslide events in central and northern Italy". In: Jansà A. & Romero R. (eds.), *Proceedings 4th Plinius Conference on Mediterranean Storms*, Mallorca, Spain, Universitat de Illes Balears, CD-ROM, ISBN 84-7632-792-7. 2003.
- [5] E. L. Harp, and R. L. Jibson, "Landslides triggered by the 1994 Northridge, California earthquake", *Seismological Society of America Bulletin*, vol. 86, pp. S319-S332. 1996.
- [6] P. S. Lin, J. Y. Lin, H. C. Hung, and M. D. Yang, "Assessing debris flow hazard in a watershed in Taiwan". *Engineering Geology*, vol. 66, 295-313. 2002.
- [7] T. R. Martha, N. Kerle, V. Jetten, C. J. vanWesten, and K. Vinod Kumar, "Characterising spectral, spatial and morphometric properties of landslides for semi-automatic detection using object-oriented methods", *Geomorphology*, vol. 116(1-2), 24-36. 2010.
- [8] G. Metternicht, L. Hurni, and R. Gogu, "Remote sensing of landslides: An analysis of the potential contribution to geo-spatial systems for hazard assessment in mountainous environments", *Remote Sensing Environment*, vol. 98, 284-303. 2005.
- [9] M. Nagao, T. Matsuyama, and Y. Ikeda, "Region extraction and shape analysis in aerial photos", *Computer Graphics and Image Processing*, vol.10, 195-223. 1979.
- [10] J. W. Rouse, R. H. Haas, J. A. Schell, and D.W. "Deering, Monitoring vegetation systems in the Great Plains with ERTS", *Proceedings of the Third Earth Resources Technology Satellite-1 Symposium*, NASA, Greenbelt, MD (1974), pp. 301-317. 1974.
- [11] W. Zhou, G. Huang, A. Troy, and M. L. Cadenasso, "Object-based land cover classification of shaded areas in high spatial resolution imagery of urban areas: A comparison study", *Remote Sensing of Environment*, vol. 113, 1769-1777. 2009.